Investigational New Drugs
https://doi.org/10.1007/s10637-018-0620-y

PRECLINICAL STUDIES

Euphol, a tetracyclic triterpene, from *Euphorbia tirucalli* induces autophagy and sensitizes temozolomide cytotoxicity on glioblastoma cells

Viviane A. O. Silva[1] · Marcela N. Rosa[1] · Vera Miranda-Gonçalves[2,3] · Angela M. Costa[2,3] · Aline Tansini[1] · Adriane F. Evangelista[1] · Olga Martinho[1,2,3] · Adriana C. Carloni[1] · Chris Jones[4,5] · João Paulo Lima[6] · Luiz F. Pianowski[7] · Rui Manuel Reis[1,2,3]

Received: 27 February 2018 / Accepted: 7 June 2018

Summary

Glioblastoma (GBM) is the most frequent and aggressive type of brain tumor. There are limited therapeutic options for GBM so that new and effective agents are urgently needed. Euphol is a tetracyclic triterpene alcohol, and it is the main constituent of the sap of the medicinal plant *Euphorbia tirucalli*. We previously identified anti-cancer activity in euphol based on the cytotoxicity screening of 73 human cancer cells. We now expand the toxicological screening of the inhibitory effect and bioactivity of euphol using two additional glioma primary cultures. Euphol exposure showed similar cytotoxicity against primary glioma cultures compared to commercial glioma cells. Euphol has concentration-dependent cytotoxic effects on cancer cell lines, with more than a five-fold difference in the IC_{50} values in some cell lines. Euphol treatment had a higher selective cytotoxicity index (0.64–3.36) than temozolomide (0.11–1.13) and reduced both proliferation and cell motility. However, no effect was found on cell cycle distribution, invasion and colony formation. Importantly, the expression of the autophagy-associated protein LC3-II and acidic vesicular organelle formation were markedly increased, with Bafilomycin A1 potentiating cytotoxicity. Finally, euphol also exhibited antitumoral and antiangiogenic activity in vivo, using the chicken chorioallantoic membrane assay, with synergistic temozolomide interactions in most cell lines. In conclusion, euphol exerted in vitro and in vivo cytotoxicity against glioma cells, through several cancer pathways, including the activation of autophagy-associated cell death. These findings provide experimental support for further development of euphol as a novel therapeutic agent for GBM, either alone or in combination chemotherapy.

Keywords Glioblastoma · Anticancer · Cytotoxic activity and euphol

Electronic supplementary material The online version of this article (https://doi.org/10.1007/s10637-018-0620-y) contains supplementary material, which is available to authorized users.

✉ Rui Manuel Reis
ruireis.hcb@gmail.com

[1] Molecular Oncology Research Center, Barretos Cancer Hospital, Barretos, São Paulo 14784 400, Brazil

[2] Life and Health Sciences Research Institute (ICVS), School of Medicine, University of Minho, 4710-057 Braga, Portugal

[3] ICVS/3B's - PT Government Associate Laboratory, 4806-909 Braga, Guimarães, Portugal

[4] Division of Molecular Pathology, The Institute of Cancer Research, London, UK

[5] Division of Cancer Therapeutics, The Institute of Cancer Research, London, UK

[6] Medical Oncology Department, AC Camargo Cancer Center, São Paulo 01509-010, Brazil

[7] Kyolab laboratório de pesquisa Farmacêutica Ltda, Valinhos, São Paulo 13273-105, Brazil

Published online: 22 June 2018

Introduction

Gliomas account for more than 70% of central nervous system (CNS) tumors. They are the second most frequent pediatric tumor in the world and therefore considered a major public health problem [1, 2]. Glioblastoma (GBM) is classified by the World Health Organization as a grade IV tumor, and it is biologically the most aggressive of the gliomas. GBM is the most frequent glioma subtype accounting for about 65% of cases [2–4] and the tumor may manifest at any age, but typically has a peak incidence of between 45 to 75 years of age [5–7]. GBMs are lethal tumors, with a median survival of about 14 months with less than 10% of patients surviving for two years following diagnosis (http://www.cancer.org; http://www.cbtrus.org) [3, 8].

The aggressive behavior of GBMs is in part due to a combination of intense cellular proliferation, diffuse infiltration, increased resistance to cell death, and high levels of angiogenesis [9, 10]. Thus, in addition therapy for GBM includes a combination regimen of radiotherapy and adjuvant chemotherapy with temozolomide (TMZ) [8]. Despite this multimodal approach, GBM usually responds poorly and prognosis has only slightly improved with time [3, 8]. Therefore, research and development of new sources of drugs with promising therapeutic findings and fewer side effects are urgently needed for GBMs.

Bioactive plants or their extracts are rapidly emerging as an alternative source of novel anti-cancer drugs. Importantly, natural products can have high antitumoral efficiency without some of the harmful side effects of conventional chemotherapies [11]. An example is resveratrol (3,4,5-trihydroxy-transstilbene) is a polyphenolic phytoalexin widely present in plants [12]. This compound exerts beneficial functions in normal cells and has been reported to be cytotoxic for the majority of malignant cells, blocking some stages of carcinogenesis in several types of cancer cells and models, including GBM [12–14].

Traditional healers use extracts of plant species from the genus *Euphorbia* (Euphorbiaceae) for the treatment of ulcers, warts, cancer and other diseases. For instance, euphol is a tetracyclic triterpene alcohol and the main constituent found in the sap of *E. tirucalli,* showing anti-inflammatory, antiviral activities, analgesic effect as well as antinociceptive properties [15–18]. Some plants of this family have also been tested for their antineoplastic activity; however, the biological impact has not been well explored, with some reports in breast and gastric tumor cell lines, which showed that euphol could decrease cell viability [19, 20].

In a previous study, we assessed the antineoplastic potential of euphol in a large panel of commercial cancer cell lines, including glioma cell lines [15]. We found that euphol has a promising cytotoxicity effect against several cancer cell lines, and significantly inhibited cell motility and migration, proliferation, and anchorage-independent growth of pancreatic cancer cell lines [15]. However, to the best of our knowledge, no studies have reported the mechanism of euphol action and its biological effect in gliomas.

Therefore, in the present study, we expanded our previous toxicological screening by investigating the therapeutic potential of euphol on primary glioma cells and by analyzing the signaling pathways and the specific cellular effects of the drug.

Material and methods

Cell lines and cell culture

Twelve immortalized human cell lines, comprising seven adult and five pediatric glioma cells lines, two primary cultures and one normal human astrocyte were used to perform cytotoxic assays. All the cell lines were maintained in Dulbecco's modified Eagle's medium (DMEM 1×, high glucose; Gibco, Invitrogen) supplemented with 10% fetal bovine serum (FBS) (Gibco, Invitrogen) and 1% penicillin/streptomycin solution (Gibco, Invitrogen), at 37 °C and 5% CO_2. Conditions and cell line origins are indicated in Supplementary Table 1. Additionally, two primary tumor cell lines, HCB2, and HCB149, derived from surgical glioblastoma biopsies obtained at the Neurosurgery Department of the Barretos Cancer Hospital (São Paulo, Brazil) were used [21, 22]. The local ethics committee approved the study protocol, and patients signed an informed consent form. The isolated cells were grown in DMEM medium under the same conditions described above. Authentication of all cell lines was carried out by the Diagnostics Laboratory at the Barretos Cancer Hospital (São Paulo, Brazil) as reported [15, 23]. Identification of the established primary culture confirmed that both primary culture and blood derived from the same patient.

Preparation and compound dilution

The euphol purification process, biochemical characterization, and dilution were carried out as described previously [15, 24]. The chemical structure of the euphol, represented in Fig. 1a was determined by elemental analyses of 1H NMR and 13C NMR spectral data, and by comparison with their respective authentic compounds using ChemDraw software version 7.0 [24] (PubChem CID: 441678). The tetracyclic triterpene euphol used in this study showed >95% purity. The drug euphol was provided by Amazônia Fitomedicamentos Ltda, which is the sole and exclusive owner of the respective intellectual property rights.

The extract fraction was initially dissolved in dimethyl sulfoxide (DMSO) at a concentration of 50 mg/mL and stored at

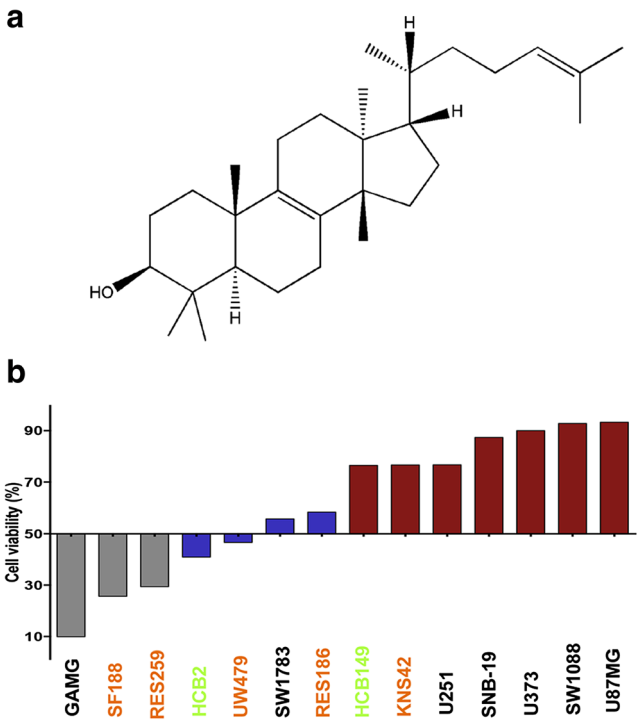

Fig. 1 Effect of euphol on cell viability of commercial and glioma primary culture. a Euphol chemical structure. **b** Cytotoxicity profile of 14 human glioma cell lines, exposed to euphol compound. Bars represent the cell viabillity at 15 μM of euphol. Colors represent the GI score classification and cancer cell lines sbgroups. Gray (HS = Highly sensitive); Blue (MS = Moderate Sensitive); Red (R = Resistant); Black (Adult glioma cell line); Orange (Pediatric glioma cell line) and Green (glioma primary culture)

−20 °C. The intermediate dilutions of the experimental compound were prepared to obtain a concentration of 1% DMSO.

Cell viability and proliferation assay

The cytotoxicity effect of euphol was assessed by Cell Titer 96 Aqueous cell proliferation assay (MTS assay-PROMEGA), and the proliferation effect was evaluated by ELISA-BrdU assay (Roche Applied Science, Mannheim, Germany), following the manufacturer's instructions as previously described [15, 23]. Cells were plated into 96-well plates (until a maximum 5×10^3 cells/well) and treated with increasing concentrations of the euphol diluted in DMEM (0.5% FBS) or vehicle (1% DMSO, final concentration) for 72 h. Half-maximal inhibitory concentration (IC_{50}) data were evaluated using the non-linear regression curve using GraphPad PRISM version 5 (GraphPad Software, La Jolla California USA), as previously determined [15, 23]. Also, the proliferation effect was assessed two hours before the end of incubation by ELISA-BrdU assay kit (Roche, Applied Science, Mannheim, Germany) following the manufacturer's instructions.

Moreover, in our screening, we adopted the criteria of growth inhibition (GI) to allow classifying the cell line profiles [25]. GI was calculated as a percentage of untreated controls, and its values were determined at a fixed dose of 15 μM (concentration that corresponds approximately to the average IC_{50} value of all cell lines at screening). Samples exhibiting more than 60% growth inhibition in the presence of 15 μM euphol were classified as highly sensitive (HS); as resistant when showing less than 40%; and as moderately sensitive (MS) when showing between 40 and 60% growing inhibition. All the assays were done in triplicate and repeated at least three times.

Selectivity index (SI)

The selectivity index for the cytoxicity of euphol was expressed as the ratio between the IC_{50} value on the normal human astrocyte cell line (NHA) and the IC_{50} value on each cancer cell line (SI=IC_{50} normal cell/IC_{50} cancer cell). Values greater than or equal to 2.0 are considered to be an important selectivity index [26].

Wound healing migration and invasion assay

Cell migration properties of GAMG, and U373 cell lines were evaluated by wound healing assay as previously described by our group [21]. The images shown are representative of three independent experiments performed in triplicates. **C**ell invasion assay in GAMG and U373 cells was performed using 24-well BD Biocoat Matrigel Invasion Chambers, according to the manufacturer's instructions (354,480, BD Biosciences) [21].

Cell cycle and apoptosis assays

Cell cycle and apoptosis assays were assessed by flow cytometry as previously described [27]. In brief, the cells were plated onto a six-well plate at a density of 1×10^6 cells/ well, allowed to adhere for at least 24 h and serum starved for 12 h. Additionally, the cells were exposed to IC_{50} concentrations values of euphol for a period of 6, 24, 48 and 72 h in DMEM (0.5% FBS). The cell cycle distribution (G1, S, and G2/M) as well as double staining with Annexin V-FITC and PI for apoptosis analysis were determined with a flow cytometer *BD FACSCanto II* (*BD Biosciences*) and analyzed with the software BD FACSDiva (*BD Biosciences*) following the manufacturer's recommended protocol. Approximately, 2×10^4 cells were evaluated for each sample in both assays.

Proteome arrays

Relative protein expression levels of a panel of 35 proteins related to apoptosis and 26 proteins related to cellular stress were obtained using the Proteome Profiler Human Apoptosis Array Kit #ARY009 (R&DSystems) and Proteome Profiler

Human Cell Stress Array Kit #ARY018 (R&DSystems), according to the manufacturer's instructions and as previously reported [21]. The selected cell lines were treated with euphol for 6 and 24 h using a concentration equivalent to an IC_{50} value of each cell line. After treatment the cells were prepared as previously described for western-blot analysis [21]. Aliquots of 500 μg of total protein were used for apoptosis proteome profile and stress human cell arrays (R&D Systems) following manufacturer's instructions.

Western blotting

To evaluate the expression of altered proteins following euphol treatment, the cells were plated onto a six-well plate at a density of 1×10^6 cells/well, allowed to adhere at least 24 h, and were serum-starved in DMEM (0.5% FBS). The cells were exposed at IC_{50} concentration values of euphol for an additional period of 6, 24, 48 and 72 h in DMEM (0.5% FBS). After the cells were prepared and aliquots of 20 μg of total protein were separated as previously described for western-blot analysis [27]. Antibodies included anti-Bip, Rip, p-27, DR5, SOD2, CytC, pP53 (S15), HSP60, HSP70, FADD and β-tubulin, all antibodies were diluted at 1:1000, (Cell Signalling Technology). In addition to PKC profile analysis, antibodies included total PKCs (PKCα, PKCδ and PKCζ), and phosphorylated PKCs; p-PKC PKDμ (S916), p-PKC PKDμ (S744), p-PKCα/βII, p-PKCpanβII, p-PKCδ, p-PKCδ/*θ*, p-PKC*θ* and PKCζ/λ, all antibodies were diluted at 1:1000 and purchased from Cell Signalling Technology.

Analysis of the autophagy process in tumor cell lines treated with euphol

The cells were plated onto a six-well plate at a density of 1×10^6 cells/ well, and allowed to adhere for at least 24 h. The growth medium was replaced by Hanks balanced salt solution (HBSS; Invitrogen) for starving the cells (two rinses in HBSS before being placed in HBSS). Then, the cells were treated with 10 nM (GAMG) and 20 nM (U373) of bafilomycin A1 (Baf), to inhibit autophagy [28]; or with euphol, using a concentration equivalent to IC_{50} of the evaluated cell line; or with a combination of Baf and euphol. All these treatments were diluted in HBSS. For autophagy assay controls, some cells were maintained in DMEM alone or treated with euphol diluted in DMEM. After 2, 6 or 24 h, the cells were scraped into cold PBS1X and subjected to western blot analysis as already described. For this, we used the primary polyclonal antibodies LC3A/B (dilution 1:1000; Cell signaling) and β-tubulin (dilution 1:5000; Cell Signaling Technology), as a loading control.

Detection and quantification of acidic vesicular organelles (AVOs) with acridine orange

To detect and quantify the AVO in euphol-treated cells, we performed the vital staining with acridine orange as reported [28]. The assay was performed according to the conditions for autophagy analysis as mentioned previously. Subsequently, 72 h after exposure to euphol, cells were removed from the plate with trypsin (Gibco, Invitrogen) and stained with acridine orange at a final concentration of 1 μg/mL for 15 min, and washed twice in PBS 1X. Green (510–530 nm) and red (>650 nm) fluorescence emission from 10^4 cells illuminated with blue (488 nm) excitation light were measured with a flow cytometer *BD FACSCanto II* (*BD Biosciences*) and analyzed in software BD FACSDiva (*BD Biosciences*). FITC-A emits green fluorescence, while PerCP-A emits red fluorescence. These analyses were performed in experimental and biological triplicates.

Analysis of the effect of the autophagy inhibitor, bafilomycin A1 (Baf), on tumor cell lines combined with euphol

To determine the effect of the autophagy inhibitor on cell viability after treatment with euphol 5×10^3 cells were plated into 96-well plates in triplicate, and increasing concentrations of euphol were added. To inhibit autophagy, fixed dose of Baf (10 nM for GAMG cells and 20 nM for U373 cells) was added to the culture 3 h after euphol treatment. The cell viability assay was evaluated after 72 h using the Cell Titer 96 Aqueous test One Solution Cell Proliferation Assay (Promega), as described by the manufacturer. Absorbance was measured on an ELISA plate (VarioskanTM-Flash, Thermo Scientific) reader at 490 nm. The data were obtained, and normalized relative to the average survival of untreated samples, or only treated with Baf. The analyses were performed in experimental and biological triplicates.

Colony formation- assay

Inhibiting anchorage-independent growth was performed using a soft-type-agar assay as previously reported [15]. We used 2×10^4 cells of GAMG and U373. The medium was changed every two days, and DMEM +0.5% FBS containing euphol at 8 and 30 μM was added. Colonies formed were stained with 0.05% crystal violet for 15 min. Photodocumented colonies were analyzed using the Image J Software. The assay was performed in two biological replicates, and the experiments were done in duplicate.

Chicken chorioallantoic membrane (CAM) assay

In vivo tumor proliferation of U373 and GAMG cell lines was assessed by CAM assay, as previously described [21, 29]. Fertilized chicken eggs were maintained at 37 °C to allow their development. On the third day, a window was made into the eggshell, allowing access to the CAM. On the tenth day of development, a small plastic ring was placed on the CAM, and 2×10^6 cells (in 20 μL DMEM- serum-free medium- Gibco Invitrogen) from U373 and GAMG cell lines were inoculated therein. The eggs were tapped and incubated. On the fourteenth day, the ring with cells was photographed *in ovo* using a stereomicroscope (Olympus S2 × 16) and a digital camera (Olympus DP71). Next, 20 μL of 0.5% FBS culture medium containing euphol (IC_{50} value) or vehicle control were injected over the tumors. On day 17 (72 h of incubation with the drug), the tumors were again photographed *in ovo*. The chickens were sacrificed by a stay at −80 °C for 10 min, and the tumors or CAM alone were fixed with 4% paraformaldehyde and photographed *ex ovo*. The perimeter of the tumors was measured using the Cell B software (Olympus) *in ovo* at days 14 and 17. The results were expressed as mean percentage of tumor growth for each group, from day 14 (considered as 0%) to day 17, ± SD. For blood vessel counting, photographs were taken at day 17 *ex ovo*, and the results were expressed as the mean of the vessels counted manually for each group of treatments ± SD. All procedures performed in studies involving animals were in accordance with the ethical standards of the institution or practice at which the studies were conducted.

Drug combination studies

Combination studies were done with fixed concentrations (determined IC_{50} value) of standard chemotherapeutic (temozolomide - Sigma - T2577), exposed to increasing concentrations of euphol. The results were expressed as mean viable cells relatively to the conditions of the fixed drug alone (considered as 100% viability) ± SD. The drug interactions were evaluated by the combination index (CI) using CalcuSyn software version 2.0 (Biosoft; Ferguson, MO, USA) [30, 31]. In CI analysis, synergy was defined as CI values significantly lower than 1.0; antagonism as CI values significantly higher than 1.0; and additivity as CI values equal to 1.0 at drug IC_{50} value for each cell line.

Statistical analysis

The results of in vitro and in vivo experiments are expressed as the mean ± standard deviation (SD) of three independent experiments and differences with $p < 0.05$ on the Student's t-test were considered statistically significant. All analyses were performed using the aforementioned GraphPad PRISM version 7 (GraphPad Software, La Jolla, CA, USA).

Results

Euphol promotes cytotoxicity and selectivity on glioma cell lines and potentiates temozolomide-induced decrease in cell viability

The antitumor effect of euphol in vitro was assessed by MTS assay in 12 glioma cell lines from commercial (adult and pediatric), primary cultures, and from one normal immortalized astrocytic cell line (Table 1). For this active extract, we generated complete dose-response curves, and calculated the IC_{50} values. There was a heterogeneous profile of response to euphol with each cell line exhibiting a distinct treatment response. The mean of IC_{50} values was 19.38 μM, but varied significantly between individual cell lines, with more than a five-fold difference in the IC_{50} values (IC_{50} range: 5.98–31.05 μM) (Table 1).

Pediatric glioma cell lines showed the most sensitive profile in comparison to primary cultures and adult glioma cell lines (IC_{50} mean 13.6, 15.3 and 24.1 μM, respectively). To a better classify the response to euphol, we adopted the criteria of growth inhibition (GI) at a fixed dose of 15 μM. This concentration was chosen because it closely corresponds to the average IC_{50} value of all cell lines at initial screening. At this fixed dose, we found that 50% (7/14) of cell lines were resistant, 28.5% (4/14) were moderately sensitive, and 21.4% (3/14) were classified as highly sensitive (Fig. 1b and Table 1). Moreover, euphol had a higher selective cytoxicity index (0.64–3.36) than TMZ (0.11 to 1.13) (Table 1).

When combined, euphol and TMZ treatments seem to have a synergistic effect (combination index (CI < 1) in 67% (8/12) of the glioma commercial cells lines investigated (mean CI values: range: 0.48–0.96) (Table 1).

Biological effect of euphol on glioma cell lines

Euphol inhibits proliferation and migration but does not impair invasion and colonies formation on glioma cells

To further explore the biological role of euphol in glioma cells, we investigated the effect of euphol selecting one drug-sensitive cell line (GAMG) and one drug-resistant cell line (U373) (Table 1). To determine whether euphol had cytotoxic or cytostatic effects on glioma cells we treated the cell lines with various concentrations of euphol for 72 h, and measured proliferation levels by BrdU incorporation. Overall, euphol exhibited dose-dependent proliferation and cytotoxicity effects on glioma cells (data not shown). The fixed dose of 15 μM of euphol inhibited 35.44% of the proliferation in GAMG and

Table 1 The euphol half maximal inhibitory concentration (IC_{50}), percentual growth inhibition (GI), the selectivity index (SI) and Combination Index (CI) of euphol against the glioma cell lines

Cell line	Euphol IC_{50} ± S.D. (μM)	Growth inhibition*	Growth inhibition score	TMZ IC_{50} ± S.D. (μM)	Euphol SI**	TMZ SI**	Combination Index (CI)*** TMZ + euphol	Primary histology
U87-MG	26.41 ± 3.19	6.7 ± 12.7	R	746.76 ± 3.15	0.76	0.15	1.11	Adult Glioma
U373	30.48 ± 3.51	10.0 ± 12.1	R	544.75 ± 1.53	0.66	0.20	0.48	
U251	29.01 ± 7.82	23.3 ± 9.5	R	696.40 ± 2.92	0.69	0.16	0.95	
GAMG	8.73 ± 1.87	90.1 ± 0.5	HS	97.00 ± 2.05	2.30	1.13	1.95	
SW1088	27.12 ± 2.55	7.2 ± 7.2	R	979.2 ± 4.00	0.74	0.11	0.70	
SW1783	19.62 ± 1.42	44.2 ± 9.6	MS	>1000±	1.02	*UD*	0.94	
SNB19	31.05 ± 5.85	12.6 ± 20.5	R	>1000±	0.64	*UD*	0.67	
RES186	16.70 ± 3.72	41.6 ± 14.8	MS	714.75 ± 7.08	1.20	0.15	1.34	Pediatric Glioma
RES259	10.34 ± 4.08	70.6 ± 8.6	HS	206.05 ± 6.09	1.94	0.53	0.52	
KNS42	19.94 ± 0.27	23.3 ± 6.2	R	>1000±	1.01	*UD*	1.10	
UW479	15.26 ± 4.83	53.4 ± 15.3	MS	>1000±	1.31	*UD*	0.92	
SF188	5.98 ± 2.42	74.4 ± 4.3	HS	>1000±	3.36	*UD*	0.96	
HCB2	11.66 ± 1.14	59.1 ± 4.0	MS	*ND*	1.72	*ND*	*ND*	Primary Glioma
HCB149	21.68 ± 5.60	23.5 ± 7.0	R	*ND*	0.92	*ND*	*ND*	
NHA	20.14 ± 4.16	47.2 ± 3.6	MS	110.5 ± 1.05				Normal Human Astrocytes

*GI was calculated as a percentage of untreated controls, and its values were determined at a fixed dose of 15 μM. Samples exhibiting more than 60% growth inhibition in the presence of 15 μM euphol were classified as highly sensitive (HS); as resistant when showing less than 40%; and as moderately sensitive (MS) when showing between 40 and 60% growing inhibition

**The selectivity index (SI) is the ratio between the IC_{50} values for NHA (Euphol IC_{50} = 20.14 ± 4.16 μM and TMZ IC_{50} = 110.5 ± 1.05 μM) and those for the glioma cell lines. *UD* = undetermined (>1000 μM); *ND* = not determined

***The CI was analyzed using CalcuSyn Software version 2.0. The CI value significantly lower than 1.0, indicates drug synergism; CI value significantly higher than 1.0, drug antagonism; and CI value equal to 1.0, additive effect

28.71% in U373 cells (Fig. 2a). Although euphol decreased the proliferation of GAMG and U373 cells, the strongest inhibition was seen at the highest applied dose of euphol (data not shown). Moreover, at 15 μM euphol suppressed cell viability of GAMG cells by 88.86% and U373 cells by 13.9% (Fig. 2b). Thus, these data suggest that euphol seems to have predominantly cytotoxic effects on the anchorage-dependent growth of both malignant glioma cell lines.

Next, the impact of euphol on cellular migration was evaluated, and no significant effect was observed in GAMG cells, suggesting that euphol (8 μM - IC_{50} value) has moderate or no interference on their migratory capacity (Fig. 2c). However, euphol (30 μM - IC_{50} value) considerably reduced U373 cell migration ability at 48 and 72 h compared to untreated cells (Fig. 2d). In the GAMG cells a further 72 h were required for the wound to completely close in untreated conditions (data not shown), suggesting that these cell have an intrinsic low capacity for migration and this may be why euphol has less effect on GAMG cells than the resistant cell line (U373).

The ability of euphol to inhibit cell invasion and anchorage-independent growth was also assessed. Euphol (8 and 30 μM) did not inhibit cell invasion (Supplementary Fig. 1a, b) nor did it suppress colonies number or size in either of the glioma cell lines (Supplementary Fig. 1c, d).

Glioma cells do not undergo cell growth arrest and apoptosis upon euphol exposure

To understand the biological mechanism of euphol on cell cycle and apoptosis, we assessed changes in signaling proteins using a human apoptosis and cell stress proteome array, comprising 61 proteins related to apoptosis, cell cycle and stress signaling (listed in Supplementary Fig. 2a, b). As shown in Fig. 3a and Supplementary Fig. 2a, the cell stress proteome array assay revealed that the exposure of GAMG cells (drug-sensitive) to euphol at 6 h resulted in downregulation of the majority of the proteins in response to euphol, with the single exception of upregulation in SOD2. In contrast, in the drug-resistant cells (U373), we observed a marked reduction in BCl-2 and NF-κB1 expression and minor changes in other proteins such as HSP60 and HIF1. Remarkably, euphol increased levels of SOD2, Thioredoxin-1 and P21 CIP1 (Fig. 3a and Supplementary Fig. 2d). However, GAMG cells treated with euphol only had upregulation of P53 (S15) activation

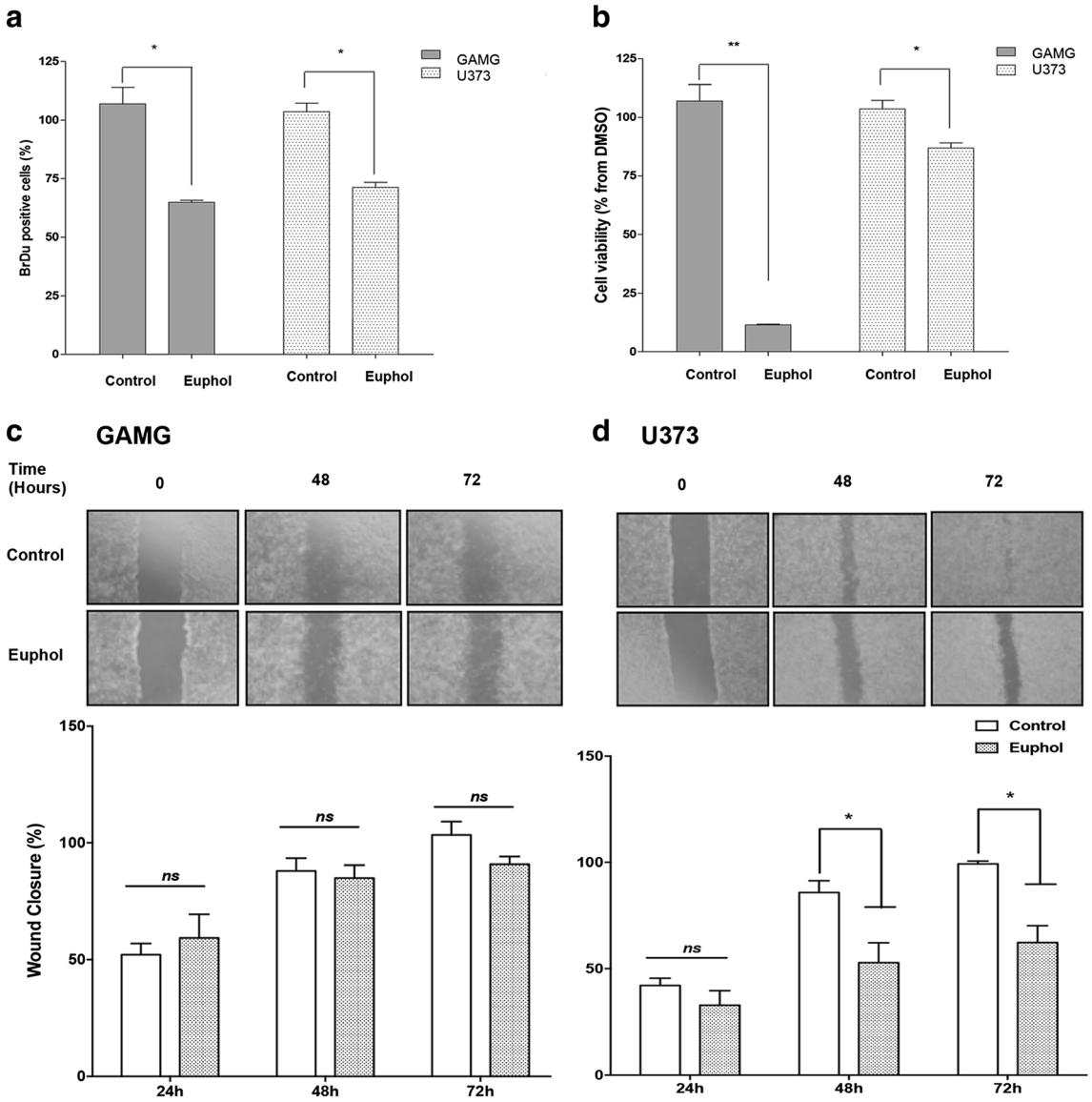

Fig. 2 Effect of euphol on glioma cell proliferation and cytotoxicity. a Cell proliferation and **b**) cell viability were measured with BrdU and MTS assay, respectively, after 72 h of euphol treatment. The proliferation of the untreated cells = 100%. Results shown are the means ± S.D. of three independent experiments. **c** GAMG and **d**) U373 cells were seeded and grown in 0.5% FBS medium containing euphol (8 and 30 μM, respectively) and evaluated by wound healing assay migration assay. A standardized scratch (wound) was applied to monolayers, and digital images were taken at several time points (0, 24, 48 and 72 h) in the same area. The distances in pixels were calculated and the percentage was calculated in time 0 h. The figures are representative of three independent experiments

and minor activation of P53 (S46) after 24 h (Fig. 3b and Supplementary Fig. 2b). In addition, euphol treatment decreased the expression of several proteins, especially: XIAP, Trail R1/DR4, Trail R1/DR5, BCL-X, and BAX while other proteins showed unchanged expression (Fig. 3b). The protein expression levels were also mostly influenced by euphol in drug-resistant cells at 24 h. Marked activation of P53 (S15), and P53 (S46) was also clearly observed in drug-resistant cells as well as upregulation of Trail R1/DR5, HSP60, and HSP70. Similarly to GAMG cells, the protein expression levels of CLASPIN, CATALASE, HIF-1, FASTNFR6/CD95 and TNRI/TNFRSF1A were particularly downregulated in U373 (Fig. 3b). These results suggest that euphol could modulate the protein profile in glioma cell lines in distinct ways.

We further examined the cell cycle distribution. FACS scanning after euphol treatment (8 and 30 μM, 72 h), showed that the cell cycle distribution (G1, S, and G2/M) of GAMG (data not shown) and U373 cells were not significantly affected (Supplementary Fig. 3a). Similarly, euphol did not appear to affect apoptosis in either GAMG or U373 cells using the same concentrations of euphol treatment evaluated by AnnexinV-FITC /PI (Supplementary Fig. 3b).

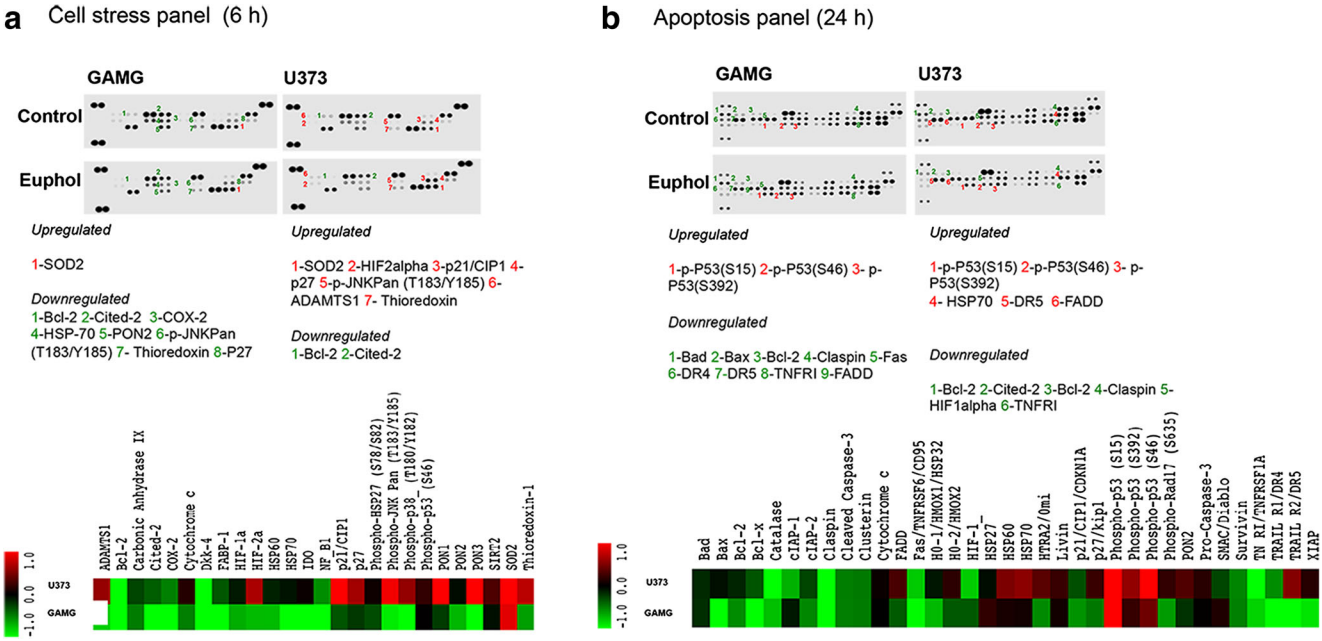

Fig. 3 Effect of euphol on cell stress and apoptosis cell in glioma cell lines. a Panel of 26 proteins related to cellular stress and **b** 35 proteins related to apoptosis. The data represented by the heat maps show the proteins modulated after 6 h (panel of cellular stress) and 24 h (panel of apoptosis) of euphol treatment (3X IC_{50} value) in glioma cells, GAMG and U373. The quantification and normalization of proteins was performed using the positive controls and untreated controls from the package *Protein Array Analyzer* of Image J software

Euphol induces autophagy in glioma cells

We next determined whether euphol could regulate autophagy cell death mechanisms, by examining the expression of the autophagy-associated protein LC3-II. Exposure to euphol (8 and 30 μM euphol) for 2 and 6 h, GAMG and U373 cells were collected and evaluated by western blotting. GAMG cells exhibited a marked increase of LC3-II compared to untreated control cells after euphol treatment either alone or when combined with Baf (Fig. 4a, b). Expression of LC3-II was especially evident following 2 h (2–fold increase) treatment. There was also significant autophagy in U373 cells treated with euphol for 2 h (data not shown). To characterize autophagy further, we performed flow cytometry after staining cells with acridine orange, a dye that detects the lysosomotropic alterations associated with acidic vesicular organelles (AVOs). Euphol treatment led to a marked increased in the acridine orange bright red fluorescence (y-axis) in U373 cells from 15.5–43.8% compared to control, indicating development of fractional volume and/or acidity of AVOs (Fig. 4c-d). To investigate euphol-induced AVOs further we performed additional experiments including the agent Baf, which is a vacuolar type H (+)-ATPase inhibitor that inhibits the fusion between autophagosome and lysosome [38]. We observed an increase of AVOs when the cells were treated either with euphol alone or when combined with Baf (GAMG 10 nM and U373 20 nM). This combination increased the formation of AVOs in U373 cells from 25.9 to 66.8% compared to Baf alone (Fig. 4d). In GAMG cells the effect was less evident (Fig. 4c). These results suggest that euphol treatment induces an increase in the development of AVOs, which is possibly associated with autophagy.

To investigate whether inhibition of autophagy at a late stage affects the cytotoxicity of euphol, we treated U373 and GAMG cells with a dose range of euphol for 72 h in the presence of a fixed dose of Baf that was added 3 h after euphol treatment. The cell viability of the euphol (350 nM) treated GAMG cells was reduced from 100 to 45% by Baf, while in U373 the cell viability was reduced from 100 to 30% with euphol (5.85 μM)

Fig. 4 Euphol induces autophagy in glioma. a) Cells were treated with ▶ IC_{50} concentrations of euphol for the indicated time periods. GAMG cell lysates (20 μg per lane) were analyzed using immunoblotting with anti-LC3. **a** and (**b**) are GAMG representative of three independent experiments. Tubulin was used as an internal control to normalize the amount of proteins applied in each lane. Development of AVO in Euphol-treated cells by detection of green and red fluorescence in acridine orange-stained cells using FACS analysis. **c** GAMG and **d**) U373 were treated with euphol (8 and 30 μM, respectively), and bafilomycin A1 (Baf) (GAMG 10 nM and U373 20 nM) for 72 h. The graphs are representative of at least two independent experiments. FITC indicates green fluorescence, while PerCP shows red fluorescence. Effect of Baf on the cell viability of euphol-treated cells. **e** GAMG **f**) U373 cells. At 3 h after exposure to euphol, baf was added and cultured until 72 h and evaluated by MTS assay. The viability of the untreated cells =100%. Results shown are the means ± S.D. of three independent experiments. Effect of Baf on euphol-induced apoptosis. After the euphol and bafilomicyn treatment for 72 h, GAMG (**g**) and U373 (**h**) cells were fixed, stained with annexinV-FITC /PI -PE and analyzed by FACScan. Data shown are representative of three independent experiments. Baf = bafilomycin A1

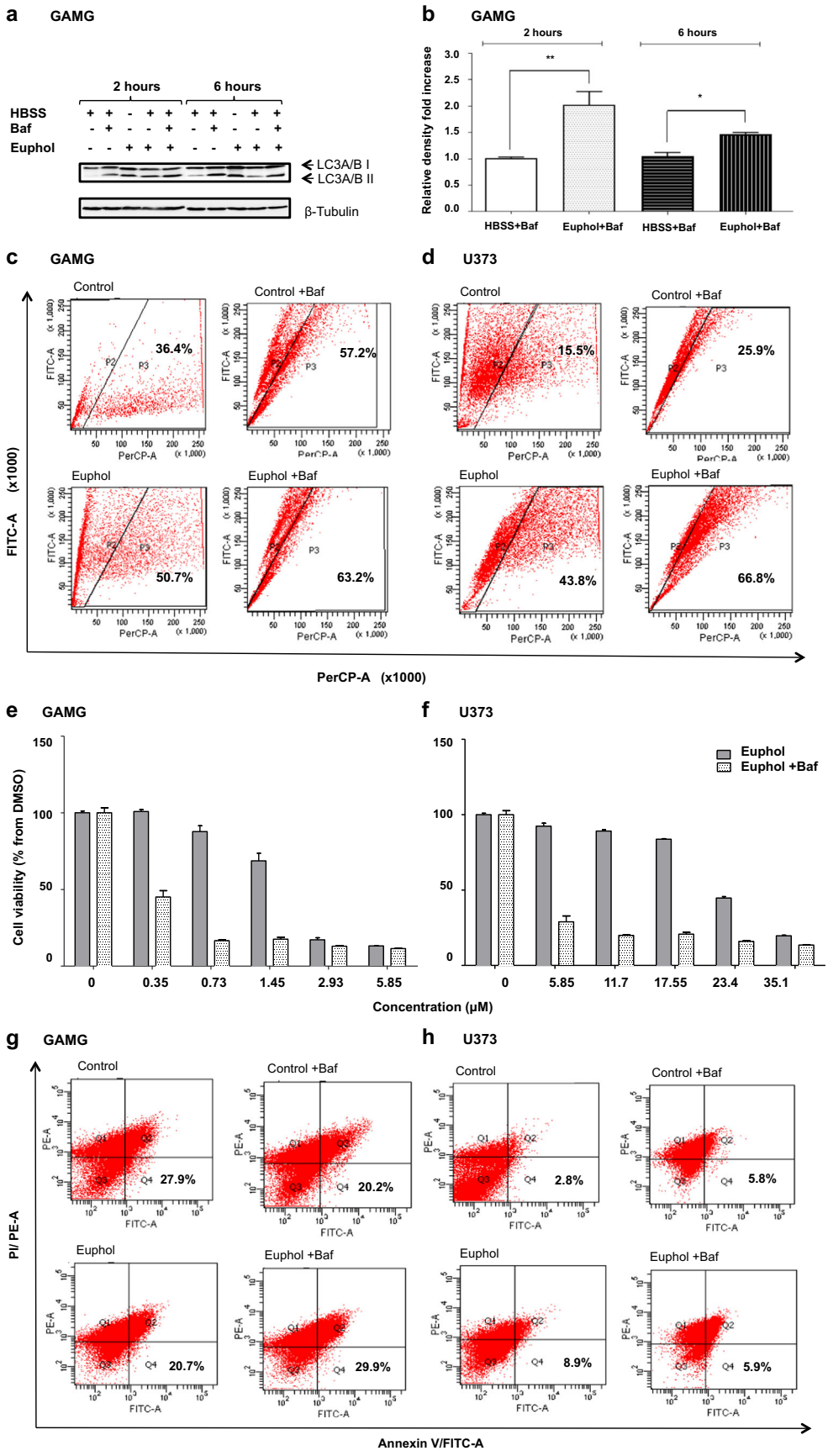
a
GAMG
2 hours
6 hours
HBSS
Baf
Euphol
LC3A/B I
LC3A/B II
β-Tubulin
b
GAMG
2 hours
6 hours
Relative density fold increase
HBSS+Baf
Euphol+Baf
HBSS+Baf
Euphol+Baf
c
GAMG
d
U373
Control
Control +Baf
Euphol
Euphol +Baf
36.4%
57.2%
50.7%
63.2%
15.5%
25.9%
43.8%
66.8%
FITC-A (x1000)
PerCP-A (x1000)
e
GAMG
f
U373
Cell viability (% from DMSO)
Euphol
Euphol +Baf
Concentration (μM)
g
GAMG
h
U373
PI/ PE-A
Annexin V/FITC-A
27.9%
20.2%
2.8%
5.8%
20.7%
29.9%
8.9%
5.9%

(Fig. 4e, f). We also investigated whether the decreased cell viability promoted by Baf in euphol treated cells was due to induction of apoptosis. However, we found that in Baf presence, euphol did not induce apoptosis (Fig. 4g, h).

Activation of the PKC signaling pathway by euphol in glioma cells

The anti-inflammatory effect of euphol in mouse skin has related to the direct inhibition of PKCα [32]. To investigate the possible role of PKC activity after treating glioma cells with euphol, we evaluated the PKC isotypes activation profile using immunoblotting. In these experiments we detected the conventional PKCs (cPKCs): PKCα, p-PKCα/βII, p-PKCpanβII, novel PKCs (nPKCs): PKCδ, p-PKCδ, p-PKCδ/θ, p-PKCθ, and atypical PKCs (aPKCs): p-PKCζ/λ, PKCζ as well as PKD1/PKCμ, p-PKC PKD (S916), and p-PKC PKDμ (S744), and no changes were observed in the status of the majority of total or phosphorylated PKC isotypes, in either of the malignant glioma cells. However, our data demonstrated that the activation of PKC/PKDμ isotypes was markedly inhibited by euphol in Ser^{744} and especially, in Ser^{916} residues during all kinetic evaluated in the U373 cells (Fig. 5b). In contrast, euphol treatment of drug-resistant U373 cells did not seem to affect PKC/PKDμ isotypes (Fig. 5a).

Effect of euphol in vivo by CAM assay

To evaluate the effect of euphol on tumor growth and angiogenesis in vivo, we performed the CAM assay. The mean perimeters of the tumors formed in the control (DMSO) and the euphol-treated cells were 1500.5 ± 265.3 μm and 1600 ± 50.4 μm, respectively, with no statistically significant differences observed in the U373 cell line (Supplementary Fig. 4). However, in euphol treated GAMG cells ($n = 19$) the mean perimeter of the tumors was reduced from 2000 μm ± 15.1 μm to 1550 ± 30.3 μm in comparison to control cells ($n = 20$) (Fig. 6a, b).

To evaluate the impact of euphol on levels of angiogenesis, we compared the number of vessels formed around the GAMG tumors in euphol-treated cells in comparison to control treated tumors. The mean number of vessels was 40 ± 5 for tumors formed by the control and 29 ± 4 for the euphol-treated GAMG cells (Fig. 6a, c). The difference in vessel densities was statistically significant suggesting that euphol treatment influenced this process. No statistically significant differences observed in the U373 cell line (Supplementary Fig. 4).

Discussion

The antitumor activity of euphol was recently reported in a large panel of 73 human cancer cell lines, including several glioma cell lines [15]. In the present study, we performed a comprehensive biological analysis of euphol, the main constituent of *E. tirucalli* sap, utilizing a panel of glioma cell lines.

The antitumor effect of euphol in vitro was studied in 10 commercial glioma cell lines, two primary cultures and one normal human primary astrocytic culture. We found that euphol treatment exhibited dose-dependent cytotoxic effects on all tested glioma cancer cell lines. In agreement with our recent study, the IC_{50} values presented were lower than 30 μg /mL for 72 h, a criterion adopted by NCI to consider an extract as promising for preclinical studies (http://www.cancer.gov) [33]. The mean of IC_{50} values was 19.38 μM (8.28 μg/mL). The glioma cell lines exhibited a heterogeneous profile of response to euphol with each cell line having a distinctive individual response. We found that 50% (7/14) of cell lines were resistant, 28.5% (4/14) were moderately sensitive, and 21.4% (3/14) were classified as highly sensitive. Pediatric glioma cell lines showed the most sensitive profile compared to primary cultures and adult glioma cell lines. This variation in response to euphol is likely a reflection of the intrinsic differences in the molecular biology underlying pediatric and adult malignant glioma [34]. The use of primary culture models for preclinical assays has recently become popular because these systems appear to mimic the genomic heterogeneity present in individual tumors [22]. In this context, our study provides additional support for the need to characterize and test new drugs using different model systems that faithfully represent tumor diversity [35].

Importantly, the euphol selectivity indexes were greater than those observed for the TMZ. Several studies have considered that a value greater than or equal to 2.0 is a selectivity index worthy of further investigation [26]. This value means that the euphol has more than twice the cytotoxicity to the tumor cell lines compared to the normal cell line for GAMG and SF188 cells, suggesting this compound is safe for further studies as a promising new therapeutic. In addition, it was not possible to calculate the selective cytotoxicity indexes for the majority of the cancer cell lines treated with TMZ since the drug is more cytotoxic to the normal reference astrocytic cell line.

Our study showed that euphol inhibition of glioma cell proliferation was concentration-dependent. Moreover, the increasing loss of cell viability at inhibitory growth concentrations suggests that its effects are more likely to be through cytotoxicity rather than a cytostatic mechanism. Our results are in agreement with our previous study [15] and with an earlier report, which also demonstrated euphol cytotoxicity in gastric cancer cell lines [20]. However, our results with glioma cells provide different findings to an earlier study using breast cancer cells [36], in which euphol was considered to modulate cell cycle proteins with cytostatic effects. Such inconsistencies may reflect the underlying biological variation of euphol in different tumor types.

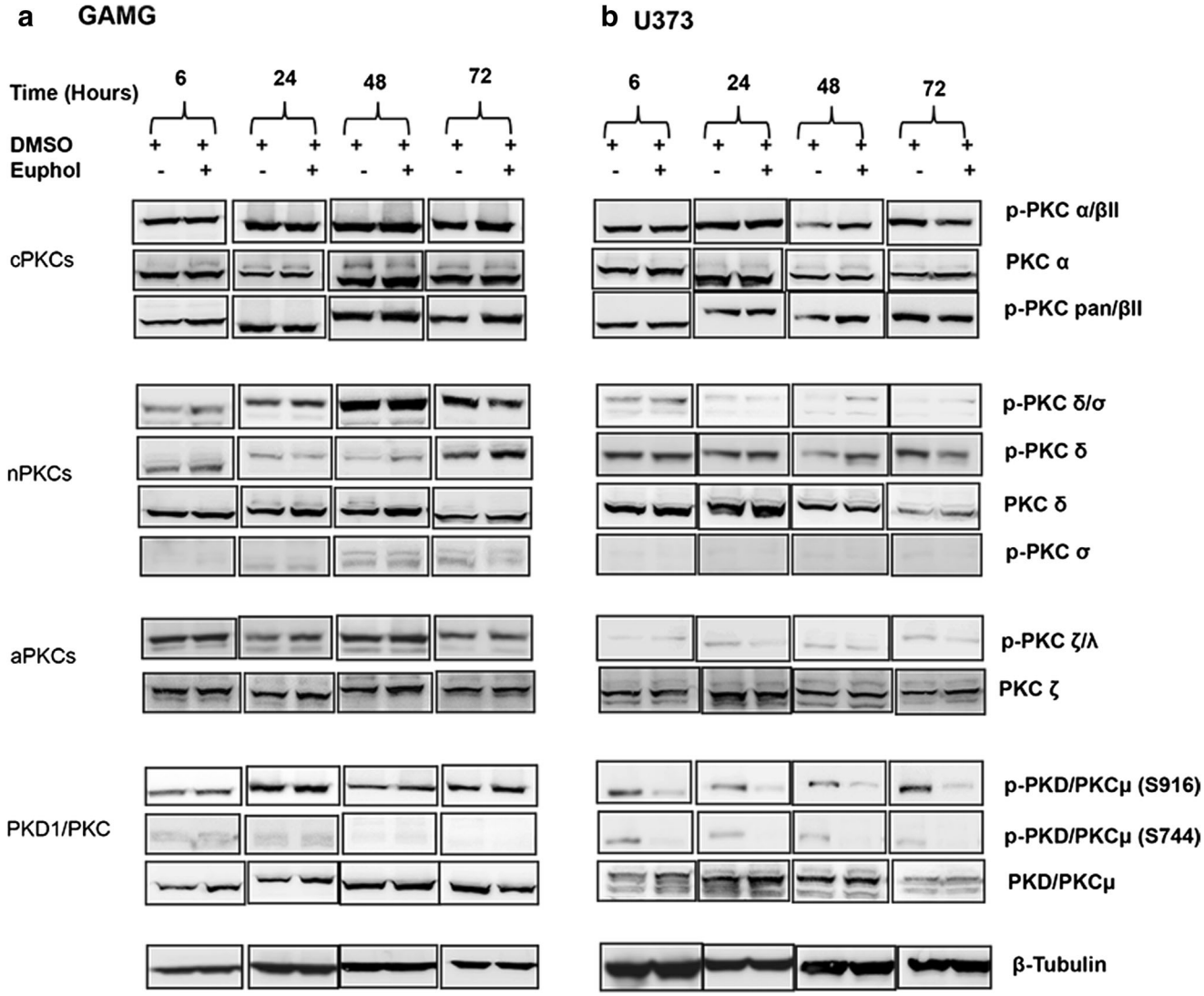

Fig. 5 Effect of euphol on PKC isoenzyme profiles in glioma cell lines. **a** GAMG and **b**) U373 cells were incubated with the IC_{50} for euphol, at 6, 24, 48 and 72 h. Controls were treated with DMSO alone (1%). Whole cell extracts from the same preparation were subjected to Western immunoblotting analysis of PKC isoenzyme expressions. Immunoblots of β-tubulin are shown as an internal control. Results shown are the means ± S.D. of two independent experiments

We further demonstrated that euphol inhibited cellular migration in U373, but not in GAMG cells. Euphol was not able to inhibit cell invasion in either of the glioma cell line analysed. Moreover, no significant effect was observed in the suppression of number and size of colonies with euphol treatment in either of the tested cell lines. There are currently no reports in the literature describing the biological effects of euphol on cancer processes such as migration and invasion, with the single exception of our study on pancreatic cancer cells [15]. These data suggest that the migration-inhibiting potential may be part of the general anti-cancer mechanism of euphol in tumorigenesis.

Next, we evaluated some of the intracellular pathways regulated by short-term exposure to euphol in glioma cells. Surprisingly, the protein expression levels in both panels of proteome arrays were the most modulated in drug-resistant cell line, U373. Moreover, we found that euphol promoted changes in anti-apoptotic and pro-apoptotic protein expression consistent with flow cytometry studies, showing that modulation of anti-apoptotic factors was more pronounced. In particular, reduced levels of pro-apoptotic BAX, BAD, TNRI/TNFRSF1A, FASTNFR6/CD95 and cleaved caspase-3 were observed for both malignant glioma cell lines and p27 and FADD in GAMG cells. In addition, antiapoptotic proteins including Livin, PON-2 and heat shock proteins were upregulated in U373 cells, in comparison to cIAP-2, Survivin, Claspin and p21 in GAMG cells. Lin and coworkers (2012) [20] observed the upregulation of the pro-apoptotic protein BAX and downregulation of the prosurvival protein Bcl-2, causing mitochondrial dysfunction, possibly by caspase-3

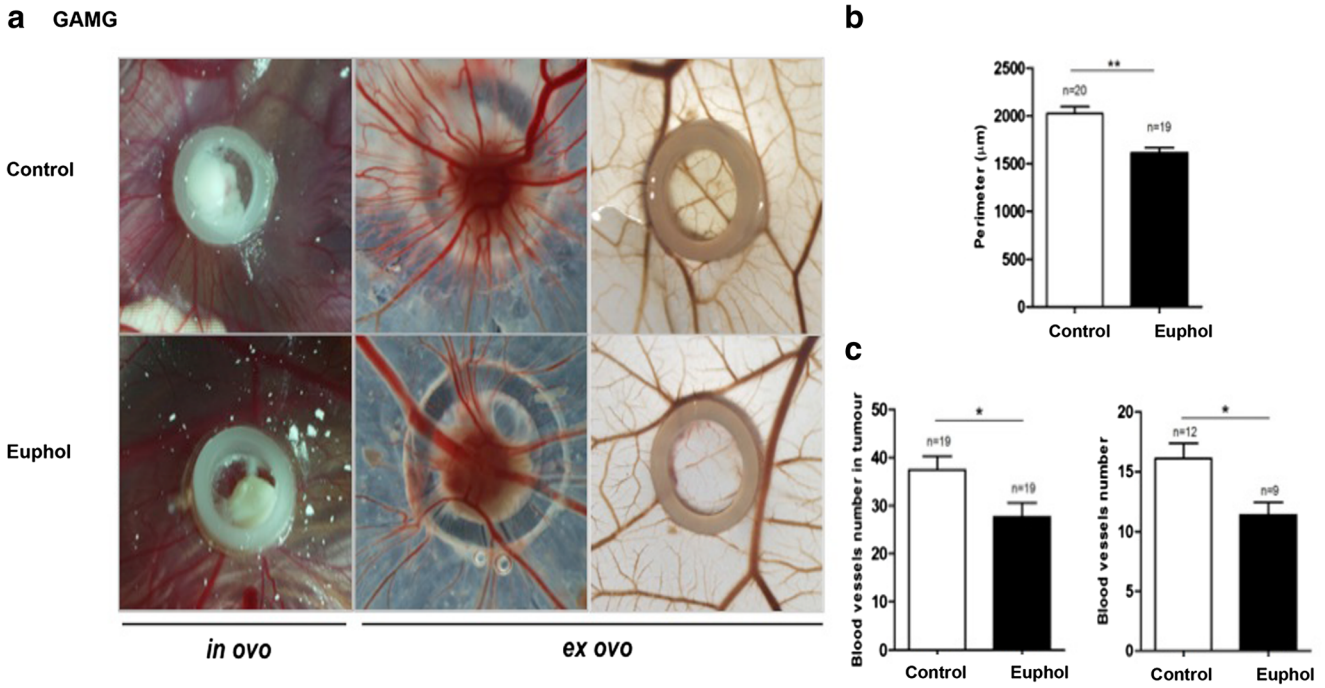

Fig. 6 In vivo role of euphol in GAMG cells growth and angiogenesis. **a** Representative images (16× magnification) of CAM assay after seven days of tumor growth *in ovo* and *ex ovo*. **b** Tumor growth was measured by perimeter (μM) in vivo by CAM assay as described in material and methods section. **c** Counting of the blood vessels *ex ovo* was performed manually by image J software. The data is represented as the mean ± SD and differences with $p < 0.05$ on the Student's t test were considered statistically significant

activation. Our data partially corroborate this study, except that BAX and caspase-3 were downregulated in both glioma cells, suggesting there may be differences in the ability of euphol to promote apoptosis in gastric cancer cells. In U373 euphol increased expression of the cyclin-dependent kinase inhibitors, p21/CIP1/CDKN1A and p27, and promoted growth arrest 6 h after exposure, with levels reducing after 24 h. In contrast, in drug-sensitive cells these proteins remained downregulated at both time-points. Wang et al. (2013) [36] reported that euphol treatment promoted up-regulation of p21 and p27 in breast cancer cells, while Lin et al. (2012) [20] found an increase of p27kip[1] levels in gastric cancer cells. These findings agree with our results from drug-resistant cells; however we did not observe marked cell cycle arrest by flow cytometry. Collectively, these results suggest that cell cycle arrest and apoptosis do not contribute to the antiproliferative and cytotoxicity effects of euphol in malignant glioma cell lines.

The induction of other non-apoptotic mechanisms of cell death such autophagy can be important for the elimination of apoptosis-resistant GBM. Our finding of a marked increase of LC3-II in euphol-treated glioma cells together with the formation of AVOs suggests that non-apoptotic processes may be activated by this compound. Moreover, the inhibition of autophagy by Baf potentiated the cytotoxicity activity of euphol in both tested glioma cell lines. Our observations are in keeping with the combinatorial effects of chemotherapeutic agents used in several clinical trials for various cancer types [19, 28]. We highlight that the application of Baf enhanced the antitumor effect of euphol against malignant glioma cells by the accumulation of autophagic vacuoles, and not by inducing apoptosis. These results are particularly important for GBM, because of this tumor has been shown to be more sensitive to agents that induce autophagy than it is to apoptosis-inducing drugs [37]. It has also been shown that autophagic structures are present in gliomas in vivo after treatments [38]. Moreover, our results agree with other studies, which have used TMZ, arsenic trioxide and berberine (natural compound) to induce autophagic cell death in malignant glioma cells, and shown that Baf enhanced the effect of TMZ and arsenic trioxide, by inducing apoptosis [39, 40]. In summary, these results suggest that autophagy plays a crucial role in the antiproliferative mechanism of euphol against glioma cells, and that inhibiting autophagy will improve the effectiveness of treatment.

The expression state of several components within the cell stress pathway was also assessed. Upregulation of the antioxidant SOD2, superoxide dismutase 2, in both cell lines should be highlighted, since this enzyme is an important defense against oxidative damage [41]. These changes indicated that euphol could promote oxidative stress by ROS induction.

Importantly, we also evaluated the isoforms of PKC. This family of protein kinases has a well-established role in oncogenesis and is one of the key targets of euphol [17].

Interestingly, while there were no changes in both glioma cell lines either in total PKC levels or in the general phosphorylation isotypes, our data demonstrated that activation of PKC/PKDμ isotypes was markedly inhibited by euphol at Ser^{744} and in U373 cells there was also strong repression at residue Ser^{916}. Functional studies have described PKD as a potent promoter of cell growth and proliferation in multiple cellular systems, suggesting that PKD may possibly contribute to the cancer phenotype [42]. PKD1 is phophorylated and active in primary glioblastoma cells and pharmacological inhibition or silencing of PKD1 by RNA-interference significantly reduced proliferation rates of glioblastoma cells in vitro [43].

We evaluated the effects of euphol on tumor growth and angiogenesis using the CAM in vitro assay. In the drug-sensitive cell line euphol exposure significantly reduced the mean perimeter of the tumors and number of the tumors vessels compared to the untreated control, whereas no statistically significance was observed in the drug-resistant cells. One possible explanation for the behaviour of U373 cells may be that euphol did not affect angiogenesis in this cell line, which could have indirectly reduced the supply of oxygen to tumor cells. Santos et al. (2016) [40] used an in vivo approach based on the ascitic Ehrlich tumor model to show that treatment with *E. tirucalli* hydroalcoholic extract led to increased survival in mice. These findings indicate the antitumoral and antiangiogenic activity of euphol in vivo. Therefore, these studies draw attention to the opportunity of investigating the effects of euphol on angiogenesis in glioma at different stages of the disease.

Importantly, we have also shown that the combined administration of euphol and TMZ exerted synergistic antitumoral action on malignant glioma cells, an effect that was also observed in tumors that are resistant to TMZ treatment. However, the GAMG cell line, which was the most sensitive to both treatments, had an antagonistic response in combinatorial therapy suggesting that an interaction, worthy of future investigation may be taking place. In general, we found that euphol promoted a synergistic antiproliferative effect (chemosensitization), with combined administration of euphol and TMZ enhancing autophagy. We, therefore, suggest that activation of autophagy plays a central role in the mechanism of action of this drug combination.

Concluding, our data provides in vitro and in vivo evidence that the plant-derived tetracyclic triterpene, euphol, exhibits potential anti-tumoral effects on glioma. Euphol administration inhibits proliferation, migration and induces autophagy-associated cell death in malignant glioma cells. Moreover, euphol enhances TMZ cytotoxic effects when given in combination and autophagy appears to have an important role, least in part, in potentiating the therapeutic effect. Our results provide a new focus for future studies, suggesting euphol as novel potent antineoplastic agent that also has therapeutic potential for adjuvant cancer treatment.

Acknowledgements The authors would like to thank Dr. Jeremy Squire for carefully proof-reading the English and for providing constructive criticism of the manuscript.

Funding The work was supported by the Amazônia Fitomedicamentos (FITO05/2012) Ltda. and Barretos Cancer Hospital, all from Brazil.

Compliance with ethical standards

Conflict of interest Viviane A O Silva declares that she has conflict of interest. Marcela N Rosa declares that she has conflict of interest. Vera Miranda-Gonçalves declares that she no has conflict of interest. Angela M Costa declares that she no has conflict of interest. Aline Tansini declares that she no has conflict of interest. Adriane F. Evangelista declares that she no has conflict of interest. Olga Martinho declares that she no has conflict of interest. Adriana C. Carloni declares that she no has conflict of interest. Chris Jones declares that he no has conflict of interest. João Paulo Lima declares that he no has conflict of interest. Luiz F Pianowski declares that he has conflict of interest. Rui M Reis declares that he has conflict of interest.

Ethical approval All applicable international, national, and/or institutional guidelines for the care and use of animals were followed. All procedures performed in studies involving animals were in accordance with the ethical standards of the institution or practice at which the studies were conducted. This article does not contain any studies with human participants performed by any of the authors.

Informed consent Informed consent was obtained from all individual participants included in the study.

References

1. Miranda-Filho A, Pineros M, Soerjomataram I, Deltour I, Bray F (2017) Cancers of the brain and CNS: global patterns and trends in incidence. Neuro-Oncology 19(2):270–280. https://doi.org/10.1093/neuonc/now166
2. Louis DN, Perry A, Reifenberger G, von Deimling A, Figarella-Branger D, Cavenee WK, Ohgaki H, Wiestler OD, Kleihues P, Ellison DW (2016) The 2016 World Health Organization classification of tumors of the central nervous system: a summary. Acta Neuropathol 131(6):803–820. https://doi.org/10.1007/s00401-016-1545-1
3. Tanaka S, Louis DN, Curry WT, Batchelor TT, Dietrich J (2013) Diagnostic and therapeutic avenues for glioblastoma: no longer a dead end? Nat Rev Clin Oncol 10(1):14–26. https://doi.org/10.1038/nrclinonc.2012.204
4. Ohgaki H, Burger P, Kleihues P (2014) Definition of primary and secondary glioblastoma–response. Clin Cancer Res 20(7):2013. https://doi.org/10.1158/1078-0432.ccr-14-0238
5. Ricci-Vitiani L, Pallini R, Biffoni M, Todaro M, Invernici G, Cenci T, Maira G, Parati EA, Stassi G, Larocca LM, De Maria R (2010) Tumour vascularization via endothelial differentiation of glioblastoma stem-like cells. Nature 468(7325):824–828. https://doi.org/10.1038/nature09557
6. Wang R, Chadalavada K, Wilshire J, Kowalik U, Hovinga KE, Geber A, Fligelman B, Leversha M, Brennan C, Tabar V (2010) Glioblastoma stem-like cells give rise to tumour endothelium. Nature 468(7325):829–833. https://doi.org/10.1038/nature09624
7. Singh SK, Clarke ID, Terasaki M, Bonn VE, Hawkins C, Squire J, Dirks PB (2003) Identification of a cancer stem cell in human brain tumors. Cancer Res 63(18):5821–5828

8. Weller M, van den Bent M, Tonn JC, Stupp R, Preusser M, Cohen-Jonathan-Moyal E, Henriksson R, Le Rhun E, Balana C, Chinot O, Bendszus M, Reijneveld JC, Dhermain F, French P, Marosi C, Watts C, Oberg I, Pilkington G, Baumert BG, Taphoorn MJB, Hegi M, Westphal M, Reifenberger G, Soffietti R, Wick W (2017) European Association for Neuro-Oncology (EANO) guideline on the diagnosis and treatment of adult astrocytic and oligodendroglial gliomas. The Lancet Oncology 18 (6):e315-e329. doi: https://doi.org/10.1016/s1470-2045(17)30194-8
9. van den Bent MJ, Smits M, Kros JM, Chang SM (2017) Diffuse infiltrating Oligodendroglioma and astrocytoma. J Clin Oncol 35(21):2394–2401. https://doi.org/10.1200/jco.2017.72.6737
10. Lieberman F (2017) Glioblastoma update: molecular biology, diagnosis, treatment, response assessment, and translational clinical trials. F1000Research 6:1892. https://doi.org/10.12688/f1000research.11493.1
11. Stupp R, Mason WP, van den Bent MJ, Weller M, Fisher B, Taphoorn MJ, Belanger K, Brandes AA, Marosi C, Bogdahn U, Curschmann J, Janzer RC, Ludwin SK, Gorlia T, Allgeier A, Lacombe D, Cairncross JG, Eisenhauer E, Mirimanoff RO (2005) Radiotherapy plus concomitant and adjuvant temozolomide for glioblastoma. N Engl J Med 352(10):987–996. https://doi.org/10.1056/NEJMoa043330
12. Filippi-Chiela EC, Villodre ES, Zamin LL, Lenz G (2011) Autophagy interplay with apoptosis and cell cycle regulation in the growth inhibiting effect of resveratrol in glioma cells. PLoS One 6(6):e20849. https://doi.org/10.1371/journal.pone.0020849
13. Pozo-Guisado E, Merino JM, Mulero-Navarro S, Lorenzo-Benayas MJ, Centeno F, Alvarez-Barrientos A, Fernandez-Salguero PM (2005) Resveratrol-induced apoptosis in MCF-7 human breast cancer cells involves a caspase-independent mechanism with downregulation of Bcl-2 and NF-kappaB. Int J Cancer 115(1):74–84. https://doi.org/10.1002/ijc.20856
14. Fuggetta MP, D'Atri S, Lanzilli G, Tricarico M, Cannavo E, Zambruno G, Falchetti R, Ravagnan G (2004) In vitro antitumour activity of resveratrol in human melanoma cells sensitive or resistant to temozolomide. Melanoma Res 14(3):189–196
15. Silva VAO, Rosa MN, Tansini A, Oliveira RJ, Martinho O, Lima J, Pianowski LF, Reis RM (2018) In vitro screening of cytotoxic activity of euphol from Euphorbia tirucalli on a large panel of human cancer-derived cell lines. Exp Ther Med. https://doi.org/10.3892/etm.2018.6244
16. Akihisa T, Ogihara J, Kato J, Yasukawa K, Ukiya M, Yamanouchi S, Oishi K (2001) Inhibitory effects of triterpenoids and sterols on human immunodeficiency virus-1 reverse transcriptase. Lipids 36(5):507–512
17. Dutra RC, Bicca MA, Segat GC, Silva KA, Motta EM, Pianowski LF, Costa R, Calixto JB (2015) The antinociceptive effects of the tetracyclic triterpene euphol in inflammatory and neuropathic pain models: the potential role of PKCepsilon. Neuroscience 303:126–137. https://doi.org/10.1016/j.neuroscience.2015.06.051
18. Dutra RC, de Souza PR, Bento AF, Marcon R, Bicca MA, Pianowski LF, Calixto JB (2012) Euphol prevents experimental autoimmune encephalomyelitis in mice: evidence for the underlying mechanisms. Biochem Pharmacol 83(4):531–542. https://doi.org/10.1016/j.bcp.2011.11.026
19. Chen N, Karantza V (2011) Autophagy as a therapeutic target in cancer. Cancer Biol Ther 11(2):157–168. https://doi.org/10.4161/cbt.11.2.14622
20. Lin MW, Lin AS, Wu DC, Wang SS, Chang FR, Wu YC, Huang YB (2012) Euphol from Euphorbia tirucalli selectively inhibits human gastric cancer cell growth through the induction of ERK1/2-mediated apoptosis. Food Chem Toxicol 50(12):4333–4339. https://doi.org/10.1016/j.fct.2012.05.029
21. Martinho O, Silva-Oliveira R, Miranda-Goncalves V, Clara C, Almeida JR, Carvalho AL, Barata JT, Reis RM (2013) In vitro and in vivo analysis of RTK inhibitor efficacy and identification of its novel targets in glioblastomas. Transl Oncol 6 (2):187–196
22. Cruvinel-Carloni A, SilvaOliveira R, Torrieri R, Bidinotto LT, Berardinelli GN, Oliveira-Silva VA, Clara CA, de Almeida GC, Martinho O, Squire JA, Reis RM (2017) Molecular characterization of short-term primary cultures and comparison with corresponding tumor tissue of Brazilian glioblastoma patients. Trans Can Res 6(2): 332–345. https://doi.org/10.21037/tcr.2017.03.32
23. Silva-Oliveira RJ, Silva VA, Martinho O, Cruvinel-Carloni A, Melendez ME, Rosa MN, de Paula FE, de Souza Viana L, Carvalho AL, Reis RM (2016) Cytotoxicity of allitinib, an irreversible anti-EGFR agent, in a large panel of human cancer-derived cell lines: KRAS mutation status as a predictive biomarker. Cell Oncol (Dordrecht) 39(3):253–263. https://doi.org/10.1007/s13402-016-0270-z
24. Dutra RC, Simao da Silva KA, Bento AF, Marcon R, Paszcuk AF, Meotti FC, Pianowski LF, Calixto JB (2012) Euphol, a tetracyclic triterpene produces antinociceptive effects in inflammatory and neuropathic pain: the involvement of cannabinoid system. Neuropharmacology 63(4):593–605. https://doi.org/10.1016/j.neuropharm.2012.05.008
25. Konecny GE, Glas R, Dering J, Manivong K, Qi J, Finn RS, Yang GR, Hong KL, Ginther C, Winterhoff B, Gao G, Brugge J, Slamon DJ (2009) Activity of the multikinase inhibitor dasatinib against ovarian cancer cells. Br J Cancer 101(10):1699–1708. https://doi.org/10.1038/sj.bjc.6605381
26. Suffness M and Pezzuto JM (1990) Assays related to cancer drug discovery. In: Hostettmann K (ed) Methods in plant biochemistry: assays for bioactivity, vol 6. Academic Press, London, pp 71–133
27. Teixeira TL, Oliveira Silva VA, da Cunha DB, Polettini FL, Thomaz CD, Pianca AA, Zambom FL, da Silva Leitao Mazzi DP, Reis RM, Mazzi MV (2016) Isolation, characterization and screening of the in vitro cytotoxic activity of a novel L-amino acid oxidase (LAAOcdt) from Crotalus durissus terrificus venom on human cancer cell lines. Toxicon 119:203–217. doi:https://doi.org/10.1016/j.toxicon.2016.06.009
28. Kanzawa T, Germano IM, Komata T, Ito H, Kondo Y, Kondo S (2004) Role of autophagy in temozolomide-induced cytotoxicity for malignant glioma cells. Cell Death Differ 11(4):448–457. https://doi.org/10.1038/sj.cdd.4401359
29. Miranda-Goncalves V, Honavar M, Pinheiro C, Martinho O, Pires MM, Pinheiro C, Cordeiro M, Bebiano G, Costa P, Palmeirim I, Reis RM, Baltazar F (2013) Monocarboxylate transporters (MCTs) in gliomas: expression and exploitation as therapeutic targets. Neuro-Oncology 15(2):172–188. https://doi.org/10.1093/neuonc/nos298
30. Bruzzese F, Di Gennaro E, Avallone A, Pepe S, Arra C, Caraglia M, Tagliaferri P, Budillon A (2006) Synergistic antitumor activity of epidermal growth factor receptor tyrosine kinase inhibitor gefitinib and IFN-alpha in head and neck cancer cells in vitro and in vivo. Clin Cancer Res 12(2):617–625. https://doi.org/10.1158/1078-0432.ccr-05-1671
31. Chou T-C, Talalay P (1984) Quantitative analysis of dose-effect relationships: the combined effects of multiple drugs or enzyme inhibitors. Adv Enzym Regul 22:27–55. https://doi.org/10.1016/0065-2571(84)90007-4
32. Passos GF, Medeiros R, Marcon R, Nascimento AF, Calixto JB, Pianowski LF (2013) The role of PKC/ERK1/2 signaling in the anti-inflammatory effect of tetracyclic triterpene euphol on TPA-induced skin inflammation in mice. Eur J Pharmacol 698(1–3): 413–420. https://doi.org/10.1016/j.ejphar.2012.10.019
33. Trendowski M (2015) Recent advances in the development of antineoplastic agents derived from natural products. Drugs 75(17): 1993–2016. https://doi.org/10.1007/s40265-015-0489-4
34. Paugh BS, Qu C, Jones C, Liu Z, Adamowicz-Brice M, Zhang J, Bax DA, Coyle B, Barrow J, Hargrave D, Lowe J, Gajjar A,

Zhao W, Broniscer A, Ellison DW, Grundy RG, Baker SJ (2010) Integrated molecular genetic profiling of pediatric high-grade gliomas reveals key differences with the adult disease. J Clin Oncol 28 (18):3061–3068. doi:https://doi.org/10.1200/jco.2009.26.7252

35. Sharma SV, Haber DA, Settleman J (2010) Cell line-based platforms to evaluate the therapeutic efficacy of candidate anticancer agents. Nat Rev Cancer 10(4):241–253. https://doi.org/10.1038/nrc2820
36. Wang L, Wang G, Yang D, Guo X, Xu Y, Feng B, Kang J (2013) Euphol arrests breast cancer cells at the G1 phase through the modulation of cyclin D1, p21 and p27 expression. Mol Med Rep 8(4):1279–1285. https://doi.org/10.3892/mmr.2013.1650
37. Kaza N, Kohli L, Roth KA (2012) Autophagy in brain tumors: a new target for therapeutic intervention. Brain Pathol (Zurich, Switzerland) 22(1):89–98. https://doi.org/10.1111/j.1750-3639.2011.00544.x
38. Lomonaco SL, Finniss S, Xiang C, Decarvalho A, Umansky F, Kalkanis SN, Mikkelsen T, Brodie C (2009) The induction of autophagy by gamma-radiation contributes to the radioresistance of glioma stem cells. Int J Cancer 125(3):717–722. https://doi.org/10.1002/ijc.24402
39. Kanzawa T, Kondo Y, Ito H, Kondo S, Germano I (2003) Induction of autophagic cell death in malignant glioma cells by arsenic trioxide. Cancer Res 63(9):2103–2108
40. Santos OJ, Sauaia Filho EN, Nascimento FR, Junior FC, Fialho EM, Santos RH, Santos RA, Serra IC (2016) Use of raw Euphorbia tirucalli extract for inhibition of ascitic Ehrlich tumor. Revista do Colegio Brasileiro de Cirurgioes 43(1):18–21. https://doi.org/10.1590/0100-69912016001005
41. Zhao P, Zhao L, Zou P, Lu A, Liu N, Yan W, Kang C, Fu Z, You Y, Jiang T (2012) Genetic oxidative stress variants and glioma risk in a Chinese population: a hospital-based case-control study. BMC Cancer 12:617. https://doi.org/10.1186/1471-2407-12-617
42. LaValle CR, George KM, Sharlow ER, Lazo JS, Wipf P, Wang QJ (2010) Protein kinase D as a potential new target for cancer therapy. Biochim Biophys Acta 1806(2):183–192. https://doi.org/10.1016/j.bbcan.2010.05.003
43. Azoitei N, Kleger A, Schoo N, Thal DR, Brunner C, Pusapati GV, Filatova A, Genze F, Möller P, Acker T, Kuefer R, Van Lint J, Baust H, Adler G, Seufferlein T (2011) Protein kinase D2 is a novel regulator of glioblastoma growth and tumor formation. Neuro Oncol 13(7):710–724. https://doi.org/10.1093/neuonc/nor084